

Production of energetic electrons during magnetic reconnection

J. F. Drake, M. A. Shay, and W. Thongthai
University of Maryland, College Park, MD 20742

M. Swisdak
Icarus Research, Inc., P. O. Box 30780, Bethesda, MD 20824-0780
(Dated: September 22, 2004)

The production of energetic electrons during magnetic reconnection is explored with full particle simulations and analytic analysis. Density cavities generated along separatrices bounding growing magnetic islands support parallel electric fields that act as plasma accelerators. Electrons because of their low mass are fast enough to make multiple passes through these acceleration cavities and are therefore capable of reaching relativistic energies.

Magnetic reconnection is the driver of solar flares, substorms in the Earth's magnetosphere and disruptions in laboratory fusion experiments. There is mounting observational evidence that a significant portion of the magnetic energy released during reconnection appears in the form of energetic electrons[9, 12]. Recent observations from the Wind spacecraft in the Earth's magnetotail suggest that electrons with energies up to 300keV are produced in the vicinity of the x-line and the distribution of energies takes the form of a power law[13]. Energetic electrons peaked around the x-line are similarly seen during the sawtooth crash and disruptions in laboratory tokamak experiments[16]. That electrons can gain as much or more energy as ions is surprising because the Alfvénic outflow velocities from the reconnection site are small compared with characteristic electron thermal velocities and the slow shocks that bound the outflow region are not expected to efficiently accelerate electrons.

In the earliest exploration of particle acceleration during magnetic reconnection the motion of test particles in fields computed from the resistive MHD model was explored[7, 11]. Initial magnetic fields were anti-parallel. The dominant energization occurred not near the x-line but within magnetic islands where locally unmagnetized particles could be both trapped and accelerated. Hoshino *et al.*, explored electron acceleration in the anti-parallel geometry with full particle simulations and showed that electron acceleration around the x-line followed by compression along the outflow produced high energy tails[5]. Acceleration in the core of islands was not a factor: the electric field in the core of magnetic islands typically remains small so in this region very little acceleration takes place. The acceleration of particles in configurations with guide fields has recently been explored[1, 3, 14]. Strong electron beams form that can drive turbulence in the form of electron-holes[1, 3]. The source of these beams are electron acceleration cavities, low density regions with non-zero parallel electric field that parallel the magnetic separatrices[14].

In this manuscript we explore the structure of these acceleration cavities and their role in the production of energetic electrons during magnetic reconnection. Upper bounds on the length of the cavities and associated elec-

tron energy are obtained. Electron energy spectra reveal a substantial population of relativistic electrons that are produced as electrons trapped in magnetic islands are able to undergo multiple accelerations. Because of the length of these cavities, a large fraction of the electrons crossing the island separatrices experience acceleration and heating. We suggest that it is the ability of electrons to circulate multiple times around magnetic islands during their growth on relatively slow ion time scales that enables electrons to gain so much energy.

The simulations are carried out with the massively-parallel PIC code p3d, which evolves the full set of Maxwell's equations with electrons and ions stepped with the relativistic Lorentz equations of motion[19]. We present the results of 2-D computations in the $x - y$ plane starting with an equilibrium consisting of two Harris current sheets with a peak density of n_0 superimposed on an ambient population of uniform density ($0.2n_0$). The system is periodic in both space directions. The reconnection magnetic field is given by $B_x = \tanh[(y - L_y/4)/w_0] - \tanh[(y - 3L_y/4)/w_0] - 1$, where $w_0 = 0.5$, $L_x = 32$ and $L_y = 16$ are the half-width of the initial current sheets and the box size in the x and y directions. The electron and ion temperatures, $T_e = 1/12$ and $T_i = 5/12$, are initially uniform as is the guide field $B_g = 1.0$. Space and time are normalized to the ion inertial length $d_i = c/\omega_{pi}$ and to the ion cyclotron time Ω_{ci}^{-1} with densities and magnetic fields normalized to n_0 and the maximum of B_x . The electron mass is $0.01m_i$, the velocity of light is 20 and the spatial grid consists of 2048×1024 cells with 100 particles per cell in the ambient background. A magnetic perturbation at the box scale is imposed to initiate reconnection.

In the double current layer configuration reconnection continues robustly until the islands from the adjacent current layers overlap. Shown in Fig. 1 are plots of the electron density, the electron temperature, the electron velocity parallel to the local magnetic field and the parallel electric field from the simulation at $t = 20.0$. The magnetic field lines point towards the left above the top island, to the right below and again to left below the bottom set of islands. The out-of-plane field points out of the figures. Density cavities with minimum values down

to 0.014 map two of the four separatrices defining each magnetic x-line (Fig. 1a). The remaining separatrices exhibit density enhancements. These cavities form as the parallel electric field (Fig. 1d) accelerates electrons along the local magnetic field toward the x-line, effectively draining the separatrix of electrons[14, 18]. The density cavities essentially map the entire separatrix in these 32×16 scale size simulations. These cavities are a nonlinear manifestation of the kinetic Alfvén wave, which mediates reconnection in the presence of a strong guide field[6, 15]. Because of the low plasma density the parallel electric field, which is normally shorted out by the parallel electron dynamics[2], remains nonzero within the cavity[14] so that the cavities become electron accelerators. In Fig. 1 this field has broken up as a result of the formation of electron-holes and double layers[1] but smoothing over these structures reveals a net “averaged” parallel electric field. Within the cavities the electrons form a beam distribution, which is evident from the large parallel velocity in these regions (Fig. 1c) combined with the low electron temperature (Fig. 1b). The beam temperature falls below the ambient electrons, a well know phenomenon in accelerator physics. The electron beams are injected into the region around the x-line where they are further accelerated and ejected outwards along the high density separatrices. The mixing of these energetic beams with cold inflowing electrons produces a very high temperature mixture in these outflow regions (Fig. 1b). Because these cavities extend along virtually the entire separatrix in the present simulations, essentially all of the electrons in the two of the four quadrants defined by the x-line undergo acceleration in the cavities and this is reflected in the increased electron temperature in the broad band of electrons within the magnetic island in Fig. 1b.

A fundamental question is whether the cavity length L_c can extend to arbitrary large distances from the x-line and what the peak velocity of electrons accelerated in these cavities is. For cavities that extend the length of the computational domain with large islands, as in Fig. 1, the acceleration region has a length $L_c \sim L_x/4$ and the peak electron velocity, including relativistic effects, is approximately given by

$$v_{\parallel} \simeq \alpha \frac{(1 + \alpha^2/4c^2)^{1/2}}{(1 + \alpha^2/2c^2)}, \quad \alpha = \left(\frac{eE_z L_x B_z}{2m_e B_x}\right)^{1/2}. \quad (1)$$

Thus, for the simulation in Fig. 1, $v_{\parallel max} \sim 14$, consistent with the measured value. In smaller simulations but with all other parameters the same, the measured maximum beam velocities were correspondingly smaller. In earlier 3-D simulations[3] the smaller value of L_x was countered by the larger value of B_z to produce the high beam velocities necessary to drive the Buneman instability.

There is a length limit of the acceleration cavities that can be determined from an upper bound on the flux of electrons flowing toward the x-line. This flux is given by the inflow across the separatrix:

$$v_{\parallel} n_c \delta y_c B_x / B \simeq v_{up} n_{up} L_c, \quad (2)$$

where δy_c and L_c are the width and length of the cavity, n_c and n_{up} are the densities inside and upstream of the cavity and v_{up} is the velocity across the separatrix into the cavity (the reconnection inflow velocity). We can relate the flux into the x-line to the jump in the out-of-plane magnetic field δB_z produced by the associated current, $v_{\parallel} n_c \delta y_c B_x / B = (c/4\pi e) \delta B_z$. The pressure from this magnetic perturbation has to be balanced either by the plasma pressure or the pressure from the in-plane magnetic field. Taking $\delta B_z / B_{z0}$ to be small, this yields an upper limit on L_c ,

$$L_c = 5d_i(1 + \beta_x)B_x/B_z, \quad (3)$$

where $\beta_x = 8\pi n(T_e + T_i)/B_x^2$, we have taken $v_{up} = 0.1c_{Ax}$, and all parameters are evaluated with their upstream values (not their cavity values). For the parameters of the simulation this is around 12, which is consistent with the length of cavities in Fig. 1a but also consistent with a cavity length limited by the computation domain. Thus, a larger simulation will be required to confirm the validity of Eq. (3). The length of the acceleration cavity can now be inserted into Eq. (1) to obtain an upper limit on the electron velocity in the cavities,

$$\alpha = c_{Axe}(1 + \beta_x)^{1/2}, \quad (4)$$

where v_{\parallel} is again given in Eq. (1) and $c_{Axe} = c_{Ax} \sqrt{m_i/m_e}$ is the electron Alfvén speed. A similar estimate for the maximum electron velocity was derived earlier with a different argument[14].

Electron energization as a result of reconnection in this simulation is not simply a result of a single pass by the electrons through the acceleration cavities. In Fig. 2 the energy distribution of electrons over the entire simulation domain is shown at three times ($t = 8.0$, $t = 12.0$, and $t = 20.0$). At $t = 20.0$ the distribution has developed a significant high energy tail that extends well above the energy associated with the cavity beams ($\sim 0.43m_e c^2$). To understand how these particles are produced we show in Fig. 3, the location of particles with energies above $1.4m_e c^2$ at $t = 20.0$. Nearly all of the energetic particles have been produced in the upper set of magnetic islands. One might guess that these particles are produced at the upper left x-line and simply free-stream along the magnetic field lines around the island. This is not the case. Shown in Fig. 4 is the energy distribution of electrons at the exit from the upper left x-line ($x, y = 12.0, 11.8$) and inside the small island at the upper left edge of the simulation ($x, y = 2.0, 11.7$). The number of electrons at the exit from the x-line drops sharply above $0.75m_e c^2$ while the spectrum of particle energies in the small island remains well-populated beyond $m_e c^2$. The most energetic particles in the simulation experience multiple interactions with the acceleration cavities. Particles are injected into the large upper x-line ($x, y = 9, 12$) from its acceleration cavities (Fig. 1d). They are then further accelerated at the x-line and follow the upper separatrix along the large upper right island. They receive an additional energy boost in the acceleration cavity at the

upper right of the simulation. These particles are finally injected into the upper left small island. The energetic particles around $x, y = 17, 9$ also came from the large upper left x-line but moved in the negative x-direction and received a second energy boost in the acceleration cavity at the bottom of the upper right island. These particles are just inside of the region of large parallel velocity seen in Fig. 1c and can be seen as a localized high-temperature region in Fig. 1b. Finally the inner band of energetic particles on the upper right of Fig. 3 came from particles ejected from the small island and that then circulated clockwise once around the upper island and underwent a second acceleration in the acceleration cavity on the upper right of the simulation domain.

The role of the small island in the upper left of the simulation in producing energetic electrons also merits discussion. Test particle calculations reveal that electrons entering this island can reach energies up to $100m_e c^2$ before their orbits become untrapped. This island is in the process of merging with the upper larger island in the simulation – note the positive value of $v_{\parallel e}$ at the x-line between the two merging islands, which is opposite in sign from that at the main x-line. The inductive electric field E_z driving the island to left appears as positive (white) on the right side of the island and negative (black) on the left hand side (Fig. 1d). For trapped electrons the electric field near the x-line on average dominates and acceleration is in the positive z direction, which is opposite in sign to the acceleration at the main x-line in the upper island chain in Fig. 1. Thus, in a system with merging secondary magnetic islands electrons can gain energy through acceleration both into and out of the plane. This is a point of some significance because the energy that can be achieved by electrons is therefore not limited to the potential drop across a finite domain in the z direction.

We have demonstrated that the multiple interaction of electrons with the low density acceleration cavities that form during magnetic reconnection with a guide field can accelerate electrons to high energies. Since the electrons in the present simulations have an artificially high mass ($0.01m_i$), electrons with more realistic masses are likely to more rapidly sample the acceleration cavities and therefore even more quickly gain energy. On the other hand, this acceleration mechanism requires the presence of multiple x-lines to be effective. A single large-scale x-line would accelerate electrons in a single pass through the cavity but would not produce the high energy particles seen here unless an alternative mechanism could be identified for scattering high energy electrons flowing away from the x-line back for further interaction with the acceleration cavities. Hoshino *et al.* have suggested that turbulence in the outflow region during anti-parallel reconnection could scatter the electrons sufficiently so that they could have multiple interactions with the x-line[5]. Although significant electric field fluctuations are present in the simulations shown here (note the bipolar structures in Fig. 1d), calculations with test particles suggest that

their amplitude is insufficient to significantly alter the trajectories of energetic electrons.

The conclusion of our work is that low-density acceleration cavities that form during reconnection are responsible for energization of a significant fraction (around 50%) of electrons crossing the separatrices during magnetic reconnection. These particles reach speeds equal to a hybrid of the electron Alfvén and electron sound speed. Multiple interactions with such cavities allow a smaller number of electrons to reach relativistic energies.

Clearly the spatial size of the simulations presented here is small compared with any natural system. Any comparison with observations requires significant extrapolations and associated uncertainties. If reconnection in the magnetotail or the sun takes place in a single large-scale x-line the present model can not explain the observations. The number of and peak energy of electrons would not be consistent with the observations. We suggest, however, that reconnection with a guide field is likely to be much more turbulent with multiple magnetic islands forming rather than a single isolated x-line, which is the norm during reconnection in the case of anti-parallel fields[17]. During guide field reconnection the electron current layers that define the magnetic x-line approach the electron Larmor scale in the transverse direction[4] and these very narrow current layers break up to form secondary magnetic islands. The small islands in the upper left and lower right regions of the simulation in Fig. 1 formed as a result of the earlier breakup of such an x-line current layer rather than as a consequence of the initial conditions. In a system with a guide field the magnetic field twists continuously and there is no preferred location for the formation of magnetic islands. In this case magnetic reconnection in a volume[8] rather than in a simple chain seems most likely. Spacecraft observations of auroral emissions from the Earth’s ionosphere reveal multi-scale patterns[10], suggesting that current layers in the magnetotail are also very highly structured, consistent with the multi-island picture. During the Wind observations of energetic particles, a substantial guide field was present and although the Earthward and tailward flows suggested a large-scale reconnection pattern, the magnetic field data revealed substantial structure[13].

A multi-island, multi-acceleration-cavity picture of electron acceleration during reconnection is consistent with several significant observations: large numbers (of the order of 50%) of electrons would undergo acceleration if the magnetic islands and acceleration cavities were of comparable size (consistent with solar observations); maximum electron energy can exceed the potential drop across the Earth’s polar cap; and a powerlaw energy distribution may be possible in a stochastic multi-island acceleration model.

This work was supported in part by DOE-MFE, NSF-Physics, NASA-SR&T and NASA-SECTP. WT was supported as part of an NSF supported REU program. JFD thanks Dr. L. Fletcher, Dr. M. Hesse, Prof. M. Hoshino, Dr. D. Longcope, Dr. P. Pritchett and other participants

at the Magnetic Reconnection Theory Program at the Isaac Newton Institute for Mathematical Sciences where

this work was completed.

-
- [1] Cattell, C., J. Dombeck, J. Wygant, J. F. Drake, M. Swisdak, M. L. Goldstein, W. Keith, A. Fazakerley, M. André, E. Lucek, and A. Balogh, in press, 2004, *J. Geophys. Res.* .
 - [2] Drake, J. F., and Y. C. Lee, 1977, *Phys. Fluids* **20**(8), 1341.
 - [3] Drake, J. F., M. Swisdak, M. A. Shay, B. N. Rogers, A. Zeiler, and C. Cattell, 2003, *Science* **299**, 873.
 - [4] Hesse, M., M. Kuznetsova, and M. Hoshino, 2002, *Geophys. Res. Lett.* **29**, 1563.
 - [5] Hoshino, M., T. Mukai, T. Terasawa, and I. Shinohara, 2001, *J. Geophys. Res.* **106**, 25979.
 - [6] Kleva, R., J. Drake, and F. Waelbroeck, 1995, *Phys. Plasma* **2**, 23.
 - [7] Kliem, B., 1994, *Ap. J.* **90**, 719.
 - [8] Li, H., *et al.*, 2003, *Phys. Plasmas* **10**, 2763.
 - [9] Lin, R. P., and H. S. Hudson, 1971, *Sol. Phys.* **17**, 412.
 - [10] Lui, A. T. Y., S. C. Chapman, K. Liou, P. T. Newell, C. I. Meng, M. Brittnacher, and G. K. Parks, 2000, *Geophys. Res. Lett.* **27**, 911.
 - [11] Matthaeus, W. H., J. J. Ambrosiano, and M. J. Goldstein, 1984, *Phys. Rev. Lett.* .
 - [12] Miller, J. A., P. J. Cargill, A. G. Emslie, G. D. Holman, B. R. Dennis, T. N. LaRosa, R. M. Winglee, S. G. Benka, and S. Tsuneta, 1997, *J. Geophys. Res.* **102**(A7), 14631.
 - [13] Oieroset, M., R. P. Lin, T. D. Phan, D. E. Larson, and S. D. Bale, 2002, *Phys. Rev. Lett.* **89**, 195001.
 - [14] Pritchett, P. L., and F. V. Coroniti, 2004, *J. Geophys. Res.* **109**(A1), 1220, doi:10.1029/2003JA009999.
 - [15] Rogers, B. N., R. E. Denton, J. F. Drake, and M. A. Shay, 2001, *Phys. Rev. Lett.* **87**(19), 195004.
 - [16] Savrukhn, P. V., 2001, *Phys. Rev. Lett.* **86**, 3036.
 - [17] Shay, M. A., J. F. Drake, B. N. Rogers, and R. E. Denton, 1999, *Geophys. Res. Lett.* **26**, 2163.
 - [18] Tanaka, M., 1996, *Phys. Plasmas* **3**, 4010.
 - [19] Zeiler, A., D. Biskamp, J. F. Drake, B. N. Rogers, M. A. Shay, and M. Scholer, 2002, *J. Geophys. Res.* **107**, 1230, doi:10.1029/2001JA000287.

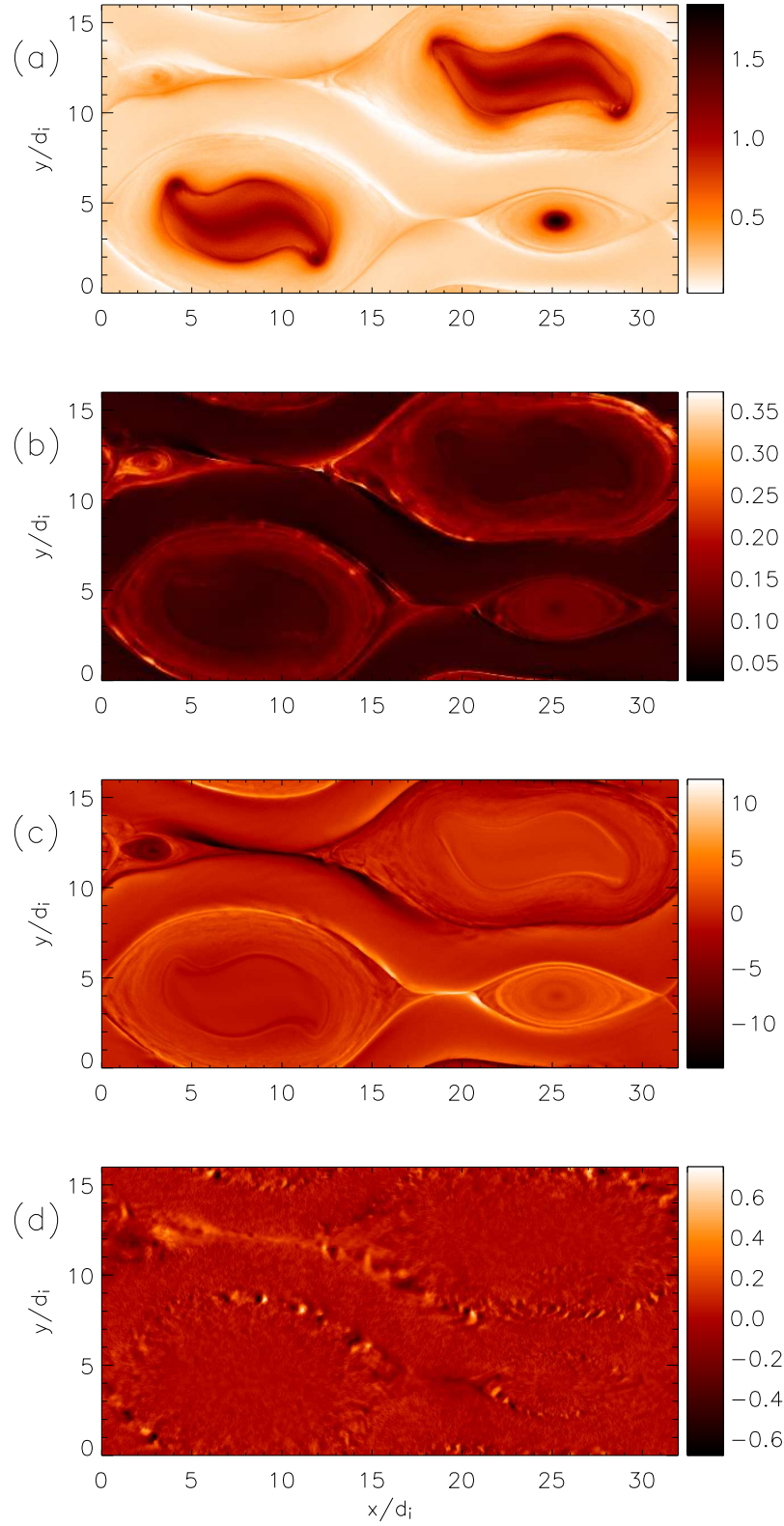


FIG. 1: Two-dimensional plots of (a) the electron density, (b) the electron temperature, (c) the electron parallel velocity and (d) the parallel electric field from a simulation with a guide field equal to the reversed field.

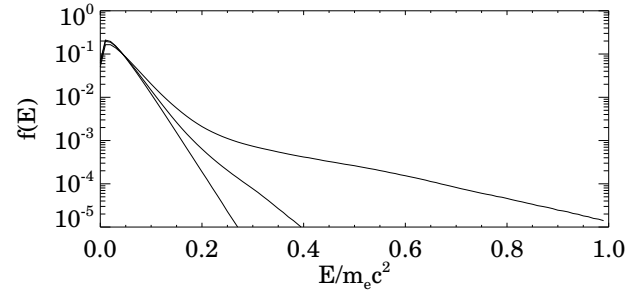


FIG. 2: Electron energy distribution from the simulation at three times: $t = 8.0$, 12.0 and 20.0 .

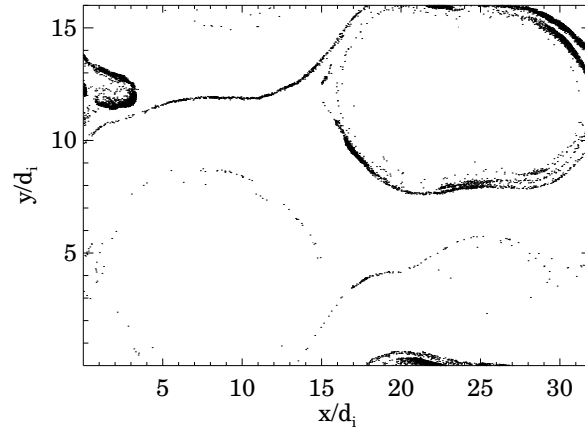


FIG. 3: Spatial distribution of electrons with kinetic energies exceeding $1.4m_e c^2$ at $t = 20.0$

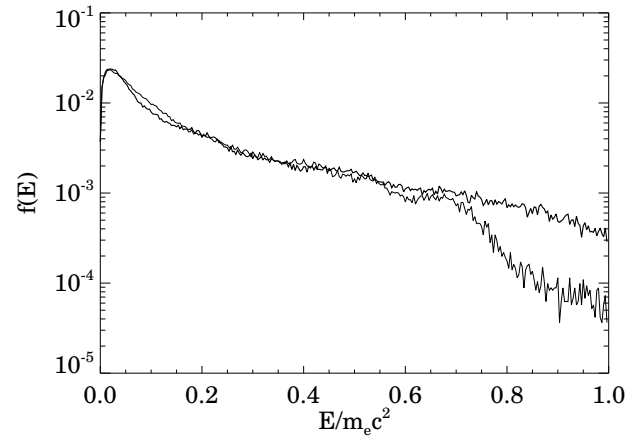


FIG. 4: Electron energy distribution at the exit from the x-line (thin) and the small island (thick) at $t = 20.0$.